Fluorine electrolysis cells: transient modelling with spatially-dependent gas properties using COMSOL®

E. Oosthuizen, G.J. Puts and P.L. Crouse*
Department of Chemical Engineering, University of Pretoria
Corner of Lynnwood Road and Roper Street, Pretoria, South Africa
*Corresponding author: philip.crouse@up.ac.za

Abstract: COMSOL Multiphysics® was used to simulate two types of laboratory fluorine electrolysis cells that operate in the temperature range 80 °C to 110 °C with nickel anodes, producing roughly 1 g of fluorine per hour. The model developed was first applied to a 2D parallel-electrode cell and then to a 3D Pauling cell geometry. The fully coupled model was prone to divergence for the 3D Pauling cell and so a unidirectionally-coupled model was applied to this 3D model. The Pauling cell comprises two tubes joined at a 90 ° angle with an electrode in each tube. The *CAD Import* module was used to import the geometry of the relevant volume from the 3D design of the cell. Prior research has shown that secondary current distribution is representative of reality and was implemented using the *Secondary Current Distribution* physics interface with Butler-Volmer kinetics. The controlled temperature of the reaction tubes is included with isothermal boundaries using the *Heat Transfer in Fluids* physics interface. An *Electrochemical Heating* multiphysics interface was added to include Joule heating of the electrolyte. The overall reaction is the electrolysis of two moles of HF into H_2(g) and F_2(g). The value of electrolyte current density at the surface of the electrodes was applied to an electron balance using Faraday's constant to determine product gas flux. A *Laminar Bubbly Flow* interface included the resulting mass and momentum transfer effects. As an improvement to all existing models in the literature, the flow of both product gases was included with the gas properties of each. The properties of the two different gas phase species were incorporated using a spatial dependency in the material definition. Mixing and temperature profiles of the cell may be investigated at different operation potentials. This model, with confirmed accuracy, may be used to avoid unnecessary laboratory experiments with hazardous chemicals and aid in accurate scale-up procedures. A modelling result for an average current density of 12 $A \cdot m^{-2}$ on the working electrode predicts an overpotential of 0.02 V and fluorine production of 0.28 $g \cdot h^{-1}$. The 2D parallel electrode implementation of the fully coupled model was successful whilst the 3D Pauling implementation still yields some numeric divergence. The 3D Pauling cell behaviour was therefore investigated using unidirectional coupling.

Keywords: Fluorine, electrolysis, electric modelling, bubbly flow

1. Introduction

The design of commercial fluorine electrolysis cells in operation in South Africa is based on technology dating essentially from the era before the proliferation of computer simulation software (Crouse 2015). The model reported here was initiated to generate a more fundamental understanding of cell operation, and to enable the rational optimisation possibility this may allow. Fluorine gas is produced commercially using a molten salt electrolysis cell (Groult 2003). Both fluorine cells and the behaviour of gaseous products in other two-phase electrolysis cells have been modelled numerically by numerous authors (Roustan, Caire et al. 1998, Hur, Shin et al. 2003, Espinasse, Peyrard et al. 2007, Mandin, Wüthrich et al. 2009, Nierhaus 2009). The previously published models greatly aid the understanding of the underlying effects on the operation of an electrolyser. These models, however, ignore either the presence or the density properties of both the product gasses as gaseous fluxes from the electrodes. A model which incorporates all the coupled physics in existing models as well as the gas properties was developed. The model was applied to the most recent investigation in the literature (Pretorius, Crouse et al. 2015) adding the presence of both product gases and is then expanded to model a 3D model of the Pauling cell (Pauling 1957: 277). The validity of spatially-dependent gas property modelling was investigated. Modelling results will be compared to laboratory data for the Pauling cell in the near future and the model will be adapted as needed as a continuing project. These models make use of nickel anodes. The complex interactions present when using carbon anodes is left for future work.

2. Physics

Cell designs

Both cells modelled in the present paper were designed and constructed at the University of Pretoria. The first of the two, with two flat, parallel electrodes, represents a common commercial geometry. The latter was designed and manufactured by the authors, based on the concept provided by Linus Pauling for laboratory use (Pauling 1957: 277).

Both cells are medium-temperature designs and have an electrolyte composition of KF·2.2HF. The operational temperature is 80 °C and both cells make use of nickel anodes (Rudge 1971: 7-14). The anodic and cathodic product gases are fluorine and hydrogen respectively.

Geometries

The geometries are shown in Figure 1 and Figure 2. In both instances the anode is depicted on the left of the figure. from the reader's point of view. The modelled geometries include only the cell internal electrolyte volume and electrodes. The typical cell configuration in Figure 1 consists of two plate electrodes submersed in the electrolyte and may be simplified to a 2D model without loss of realistic results. The Pauling cell, however, presents no exploitable symmetry elements and must be represented as a 3D geometry despite computational cost. The only intricacy to the Pauling cell geometry is at the connection of the reaction tubes to the elbow fitting. This is illustrated using the meshed representation in Figure 3.

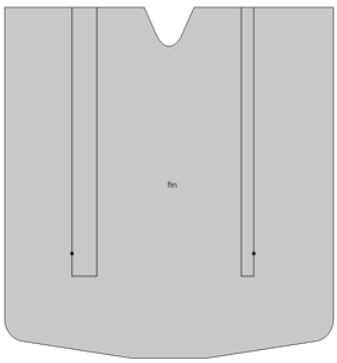

Figure 1: 2D parallel electrode modelled geometry.

Figure 2: 3D Pauling cell modelled geometry.

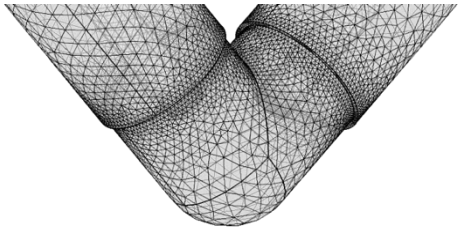

Figure 3: Geometric intricacy of the 3D geometry at elbow fitting.

Current distribution

The electrical behaviour of the cell is modelled using the *Secondary Current Distribution* physics interface. Prior research has shown that this model for current distribution is representative of reality (Roustan, Caire et al. 1998). All boundaries that are not electrode surfaces were defined as electric insulation. The anodic electrode surface is defined with an electrode reaction that employs the anodic Tafel equation. The exchange current density was set to 2×10^{-5} A·cm^{-2} and the anodic Tafel slope to

$$2.303\,\frac{RT}{0.8F} \qquad (1)$$

where R is the ideal gas constant, T is the absolute temperature at the electrode and F is Faraday's constant (Rudge 1971). A limiting current density of 100 A·cm^{-2} was employed. The limiting current density is not representative of the real mass transfer behaviour, but is a good estimate thereof. A double layer capacitance of 30 µF· cm^{-2} was included for the anode. For the cathode, kinetics were defined as thermodynamic equilibrium due to insufficient data available in the literature.

The electrical conductivity of the electrolyte was taken to be 6.67 S·m^{-1}. The anodic and cathodic electrical conductivities were taken as2.088×10^{6} S·m^{-1} and 4.032×10^{6} S·m^{-1}. The cathodic potential is specified as 0 V and the anode external circuit potential as 12 V. The reversible cell voltage at the anode is 2.9 V.

Heat transfer

Heat transfer in the cell was modelled using the *Heat Transfer in Fluids* physics as well as the

Electrochemical Heating multiphysics interfaces. For the 2D parallel electrode model the heat transfer in the solid electrodes was added. This was neglected in the 3D Pauling cell model. Table 1 includes the physical properties of the fluid applied in the physics interface. The properties applied for the electrodes in the 2D parallel electrode model are listed in Table 2.

Table 1: Physical properties for heat transfer model in electrolyte

Property	Value
Thermal conductivity ($W \cdot m^{-1} \cdot K^{-1}$)	1.25
Density ($kg \cdot m^{-3}$)	2000
Heat capacity at constant pressure ($J \cdot kg^{-1} \cdot K^{-1}$)	$10.8 + 0.00284\,T$
Ratio of specific heats	1

Table 2: Physical properties for heat transfer model in electrodes

Property	Value	
	Anode	Cathode
Thermal conductivity ($W \cdot m^{-1} \cdot K^{-1}$)	90	44.5
Density ($kg \cdot m^{-3}$)	8908	7850
Heat capacity at constant pressure ($J \cdot kg^{-1} \cdot K^{-1}$)	475	475

For the 2D parallel electrode model the sides of the cell are defined as isothermal boundaries at 80 °C. The bottom of the cell is defined as a diffuse surface with radiation to an ambient temperature of 25 °C using an emissivity of 0.26. The top of the electrolyte surface is defined as a thermal insulator.

For the 3D Pauling cell model all the electrodes and cell walls are defined as non-flux boundaries. The cell walls are defined as isothermal at 80 °C.

Fluid motion and bubbly flow

Transient bubbly flow was modelled using the *Laminar Bubbly Flow* physics interface (Pretorius, Crouse et al. 2015). This interface incorporates solution of electrolyte velocity and pressure together with phase fractions. A homogeneous flow slip model was applied for a bubble diameter of 1 mm. The density of the electrolyte was defined to be consistent with the value in Table 1. The dynamic viscosity for this phase was set as 0.01127 Pa·s. The properties of only one gaseous phase may be incorporated. To incorporate a more realistic result than was obtained in the most recent literature (Pretorius, Crouse et al. 2015), the gas phase density was defined to be spatially variant. In each model the gas phase density changes by use of a step function close to the centre between the electrode surfaces. For coordinate values smaller than the specified x-coordinate the ideal gas density of fluorine is used. For x-coordinate values greater than the specified threshold. the density of hydrogen is used.

The electrolyte surface is defined as a non-flux boundary for the liquid phase. An ambient pressure boundary condition is applied for the gaseous phase with backflow suppressed. The cell walls are non-slip and non-flux for the liquid and gaseous phases. The electrode surfaces are defined as non-slip boundaries for the liquid phase with an inward gas flux for the gaseous phase. The gaseous flux is determined using Faraday's constant to set up an electron balance using the value for local current density on the electrode surface. This flux is coupled to the presence of gaseous products shielding the electrode by multiplication with the liquid phase fraction. Equation 2 shows the *coded expression* for the anode where F is Faraday's constant, `cd.IMag` is the current density vector magnitude, `MMF2` is the molar mass of fluorine and `bf.phil` is the liquid phase fraction.

```
(cd.IMag/F)*MMF2*bf.phil        (2)
```

A zero pressure reference was defined on the 2D parallel electrode model and at the top of both reaction tubes for the 3D Pauling cell model. Gravity was added to the model together with an additional volume force in the y-direction that allows for incorporation of natural convection. The *coded expression* is given in Equation 3, where `g_const` is the gravitational acceleration constant, refers to the density of the liquid phase that the *Laminar Bubbly Flow* interface has access to, `alpha0` refers to the expansion coefficient for the electrolyte (Rudge 1971) and `T` the temperature in Kelvin.

```
g_const*bf.rho*alpha0*          (3)
(T-353.15)
```

Resolution scheme

For the 2D parallel electrode model all physics were fully coupled and successful convergence of the model obtained. For the 3D Pauling cell model repeated divergent results were obtained, which forced a unidirectional coupling of the system. Using this coupling the electrical and thermal behaviour of the cell at steady state are determined and these results used to transiently model the fluid motion and bubbly flow. Molten salt cells are known to reach a pseudo steady state after

approximately 50 s. The models were therefore computed for this time.

Mesh

Both the geometries were meshed using standard physics defined meshes generated by COMSOL Multiphysics®. Mesh dependency is still being investigated. For the results presented here a *Finer* mesh density was used for both geometries. These meshes are included in Figure 4 and Figure 5.

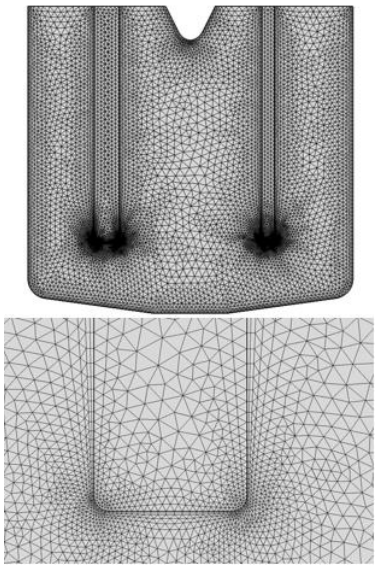

Figure 4: 2D parallel electrode geometry mesh with enlarged anodic mesh refinement.

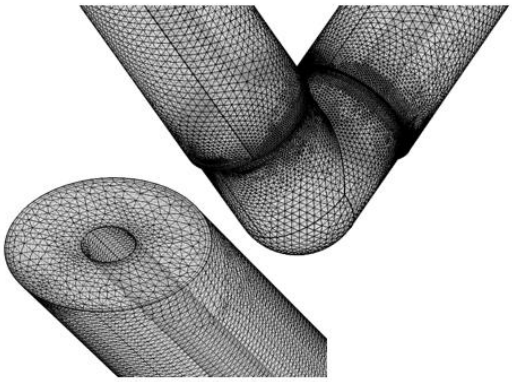

Figure 5: 3D Pauling cell geometry mesh focussed on the angle reaction jube joint and anodic outlet.

3. Results

2D parallel electrode geometry

The results obtained from the 2D parallel electrode geometry are similar to results published in the literature (Pretorius, Crouse et al. 2015). The valuable insight obtained from the new modelling attempt is that when a nickel anode is used well defined gas plumes are visible, but some entrainment of the produced fluorine in the cell's convection pattern is present. Some recombination may therefore be expected. An oscillating flow pattern depicted in Figure 6 is observed. The maximum of the colour range is fixed for comparability to the single gas property result. The maximum of the colour range should be 0.25 m·s^{-1}.

Spatially-dependent gas property may result in artificial acceleration of the mixing convection in the centre of the cell. This would be caused by the discontinuity in gas density as the gas passes over the chosen threshold. The discontinuity in gas properties is clearly visible in the gas volume fraction plot in Figure 7. A modified model was calculated to investigate the presence of artificial convection. Figure 8 shows the result obtained. The oscillating flow pattern is still visible. The lower maximum liquid phase velocity is due to the density of fluorine gas, which is more dense than hydrogen, being used.

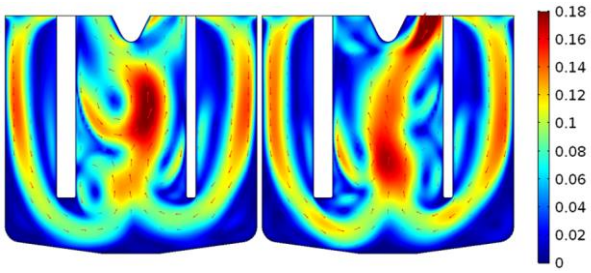

Figure 6: Liquid phase velocity magnitude (m·s^{-1}) when using spatially-dependent gas density, t = 47s; t = 48 s.

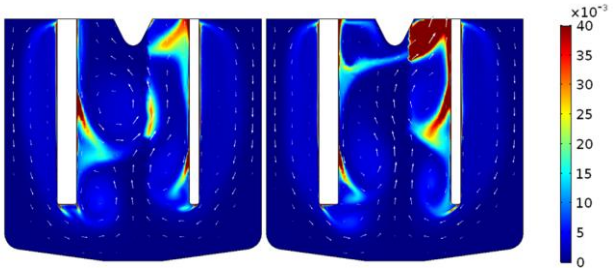

Figure 7: Gas fraction when using spatially-dependent gas density, t = 47 s; t = 48 s. Note the discontinuity in gas density.

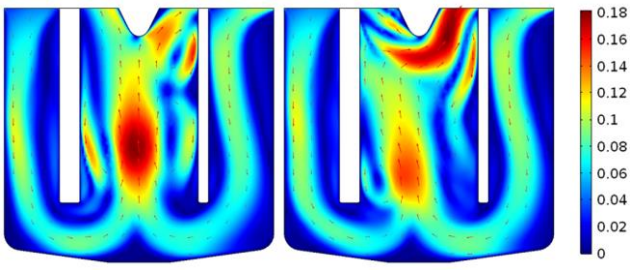

Figure 8: Liquid velocity magnitude (m·s^{-1}) when using the density of fluorine for all gas phases, t = 46s; t = 47 s.

From inspection of all the available results it is observed that the mixing in the centre of the cell is predicted to be more vigorous by using spatially-dependent gas properties.

3D Pauling cell geometry

The current distribution results are realistic. The reversible potential is visible as well as overpotential on the anode. This overpotential, shown in Figure 9, is a result of the specified limiting current density and should be compared to laboratory results. The modelling inaccuracy in neglecting a limiting current of some sort is not as easily observed in cells that approximate parallel plates. A valuable observation is that the active areas on the anode and cathode are mass transfer dependent.

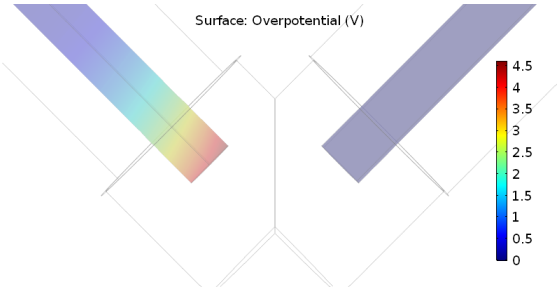

Figure 9: 3D Pauling cell geometry anodic overpotential.

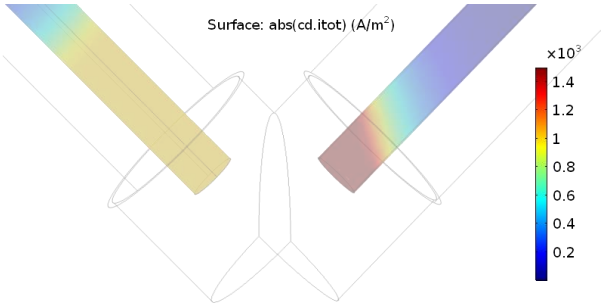

Figure 10: 3D Pauling cell geometry current density.

The gas flux resulting from the current distribution results in the gas fraction plot in Figure 11. The well developed plume of hydrogen gas evolution may be observed. The low volume fraction at the centre of the cell suggests that the small amount of recombination should not influence the fluid motion streamlines excessively. The liquid phase x-velocity magnitude is depicted in Figure 12.

From this result it may be observed that for a geometry that prevents product recombination spatially-dependent properties are a suited modelling assumption. This modelling assumption should result in more realistic fluid motion modelling than has been achieved for this system.

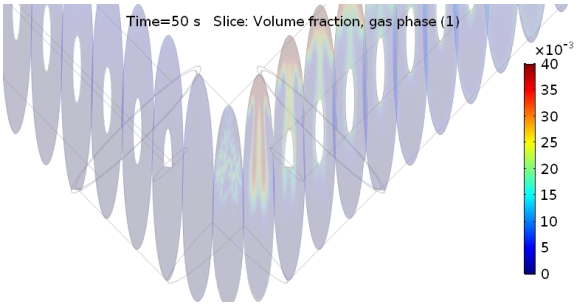

Figure 11: 3D Pauling cell geometry gas fraction plot.

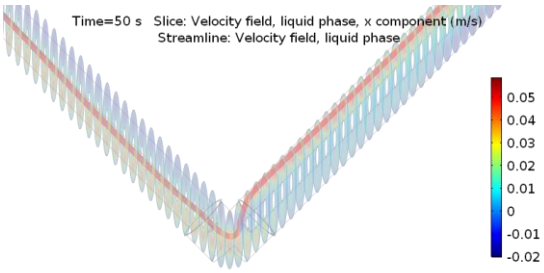

Figure 12: 3D Pauling cell geometry x-velocity magnitude and streamline.

4. Conclusions

Fully coupled modelling of a fluorine cell is possible and has been achieved by past authors. The inclusion of spatially-dependent gas properties in such a model is a novel application. This modelling assumption induces artificial cell behaviour when product gas recombination is present. When recombination is not present, more realistic flow patterns and convection modelling is expected.

Future work will include the investigation of artificial convection patterns due to spatially-dependent gas properties in cell designs that have a skirt to prevent recombination. Fully coupled modelling using a 3D Pauling cell geometry is yet to be accomplished.

References

Crouse, P. L. Fluorine: a key enabling element in the nuclear fuel cycle, *Journal of The Southern African Institute of Mining and Metallurgy* **115**: 931-936 (2015)

Groult, H. Electrochemistry of Fluorine Production, *Journal of Fluorine Chemistry* **119**: 173-189 (2003)

Roustan, H., et al. Modelling Coupled Transfers in an Industrial Fluorine Electrolyser, *Journal of Applied Electrochemistry* **28**(1998): 237-243 (1998)

Hur, J. S., et al. Modeling of the Trajectories of the Hydrogen Bubbles in a Fluorine Production Cell, *Journal of the Electrochemical Society* **150**(3): D70-D78 (2003)

Espinasse, G., et al. Effect of hydrodynamics on Faradaic current efficiency in a fluorine electrolyser, *Journal of Applied Electrochemistry* **37**: 77-85 (2007)

Mandin, P., et al. Electrochemical Engineering Modelling of the Electrodes Kinetic Properties During Two-Phase Sustainable Electrolysis. International Symposium on Process Systems Engineering. R. M. de Brito Alves, C. A. O. do Nascimento and E. C. Biscaia. Salvador-Bahia, Elsevier**:** 435-440 (2009)

Nierhaus, T. Modeling and Simulation of Dispersed Two-Phase Flow Transport Phenomena in Electrochemical Processes. Maschinenwesen, Rheinisch-Westf¨alischen Technischen Hochschule. **Doctorate Diploma in Engineering Science:** 196 (2009)

Pretorius, R., et al. A multiphysics simulation of a fluorine electrolysis cell, *South African Journal of Science* **111**(7/8): 1-5 (2015)

Pauling, L., *College Chemistry*. W H Freeman and Company, San Francisco, USA (1957)

Rudge, A. J. (1971). Production of Elemental Fluorine. Industrial Electrochemical Processes. A. J. Kuhn. Amsterdam, Netherlands, Elsevier**:** 5, 60.